A QUANTITATIVE DESCRIPTION OF QX222 BLOCKADE OF SODIUM CHANNELS IN SQUID AXONS

C. F. STARMER,* JAY Z. YEH,‡ AND JOËLLE TANGUY§
*Departments of Computer Science and Medicine (Cardiology), Duke University Medical Center, Durham, North Carolina 27710; ‡Department of Pharmacology, Northwestern University, Chicago, Illinois 60611; and §Laboratoire de Neurobiologie, Ecole Normale Superieure, Paris, France

ABSTRACT The interaction of QX222, a quaternary ammonium derivative of lidocaine, with the Na channel was studied in internally perfused squid axons under voltage-clamped conditions. A use-dependent block was observed in response to repetitive depolarizing pulses. The time constant for block development and the steady state level of the block were increased with increasing frequency of stimulation from 0.1 to 10 Hz. Use-dependent block can be viewed as a net increase in the drug incorporation into Na channels with successive pulses. That is, net drug uptake by Na channels occurs during the depolarizing phase and net drug release occurs during the interpulse interval. The observed uptake rate of use-dependent block is shown to be a linear combination of the uptake rates associated with the depolarizing and resting potentials. Also, the steady state fraction of blocked channels is shown to be a linear combination of the state-dependent blockade equilibria. Drug-channel interactions are assumed to be dependent on gated control of the diffusion path between drug pool and the interior channel binding site. Drug ingress to the binding site can be inhibited by the channel gates (receptor guarding), while drug bound to the channel may become trapped by closure of the channel gates (trapping). On the basis of these assumptions, a simple procedure is proposed for estimating apparent rate constants governing the drug-channel binding reactions for two cases of channel blockade. The estimated forward (k) and backward (l) rate constants are: $2.45 \times 10^5\ M^{-1}\ s^{-1}$ and $0.23 \times 10^3\ s^{-1}$, respectively, for k and l for the case when the drug is trapped by both activation and inactivation gates, and $3.58 \times 10^5\ M^{-1}\ s^{-1}$ and $4.15 \times 10^{-3}\ s^{-1}$ for the case when the drug is not trapped. While these two schemes make a similar prediction with respect to the resulting uptake rates, their prediction of the steady state level of block differs. The observed steady state level of block could quantitatively be predicted by the trapped scheme but not by the untrapped scheme, thus providing a means for discriminating between these two schemes. In addition, the trapped scheme, but not the untrapped scheme, could provide an explanation for the observed voltage dependence of the slow recovery from use-dependent block.

INTRODUCTION

Local anesthetics block Na channels in many excitable membranes, including frog node of Ranvier (Strichartz, 1973), squid giant axon (Cahalan, 1978; Yeh, 1978), and cardiac muscle (Hondeghem and Katzung, 1977). The block may show frequency dependence as well as voltage dependence (Strichartz, 1973; Courtney, 1975). The voltage dependence arises from two sources: interaction between drug charge and membrane potential (Strichartz, 1973; Yeh, 1982; Starmer et al., 1984), and voltage-sensitive gating kinetics that control drug access to the channel binding site thought to reside within the channel interior (Strichartz, 1973; Hille, 1977). The frequency-dependent pattern of channel blockade results from a variation in the period of time available between stimuli for drug to diffuse out of the channel. Thus, drugs with unbinding time constants less than one-fourth the interstimulus interval will not show use dependence.

This paper presents a quantitative description of Na channel blockade by QX222 that considers the binding site as transiently accessible, and explicitly includes the effects of gate-trapping of drug within the channel interior (Strichartz, 1973; Yeh, 1979; Yeh and Tanguy, 1985). The description of transient binding site accessibility is based on gated control of drug ingress to and egress from the binding site (Starmer et al., 1984; Starmer and Hollett, 1985). Here we show that by approximating the stochastic gate behavior with synchronized openings and closings, such that all channel gates open together and are open for a period equal to the mean receptor access time, a simple, quantitatively accurate model of blockade can be derived. On the basis of this characterization, a method for estimating the apparent rate constants is presented along with a test for whether or not the drug is trapped during the recovery interval. When the receptor access time is large, the resulting theoretical description is equivalent to that describing interactions between ligands and continuously accessible receptors.

METHODS

Experiments were performed on giant axons isolated from squid, *Loligo pealei*, obtained at the Marine Biological Laboratory, Woods Hole, MA. Axons were internally perfused with the roller method (Baker et al.,

1961) and voltage-clamped with an axial wire electrode assembly. We used two sets of guard electrodes on either side of the axon and air gaps on either end to improve the space clamp as described by Oxford (1981). The rise time of the clamp was 3 μs (10–90% step command pulse). Feedback compensation was used in all experiments to compensate for errors arising from approximately two-thirds of the measured 3–4 Ω · cm² of series resistance. The axons were perfused externally with artificial seawater containing ions in the following concentrations (mM): 450 Na^+, 50 Ca^{2+}, 10 HEPES buffer, 550 Cl^-. The pH of the external solution was adjusted to 8.0 and its osmolarity to 1,000 mosmol. The internal solution was composed as follows (mM): 50 Na^+, 275 Cs^+, 275 glutamate$^-$, 50 F^-, 400 sucrose, 15 phosphate buffer, adjusted to a pH of 7.3 and an osmolarity of 1,040 mosmol. Drugs were internally applied to internally perfused axons. QX222 was generously supplied by Dr. B. Takmann of Astra Pharmaceutical Products, Worcester, MA. All experiments were performed at a temperature of 8.5 ± 0.5°C.

The time course of channel blockade was assessed at a concentration of 2 mM QX222 using a train of 10 10-ms depolarizing pulses to 0 mV, given at rates of 0.1, 0.2, 0.25, 0.33, 0.5, 1, 2, 2.5, 4, 5, and 10 Hz, and from a holding potential of −80 mV.

Analytical Methods

We view ion channel blockade as a bimolecular interaction between unblocked channels, U, and drug, D, where the diffusion paths between drug pools and the binding sites are controlled by the channel gate proteins. Drug ingress to the binding site may be inhibited by closed channel gate conformations (receptor guarding), while drug bound to the interior binding site may become trapped within the channel by gate closure (trapping). The gated bimolecular process is defined by

$$U + D \underset{gl}{\overset{fk}{\rightleftharpoons}} B$$

where f is the fraction of unblocked channels with accessible binding sites and g is the fraction of blocked channels where the drug is untrapped and thus free to unbind. Guarding has been described earlier by Strichartz (1973), Courtney (1975), Hille (1977), Yeh (1978), and Starmer et al. (1984), and trapping has been described by Strichartz (1973), Schwarz et al. (1977), Yeh (1978), Yeh and Tanguy (1985), and Starmer et al. (1984). Using the Hodgkin-Huxley (1952) gating formalism, we postulate that for hydrophilic agents, $f = m^3h$ and $g = m^3h$; for hydrophobic agents, $f = m^3$ and $g = 1$. Blockade is described by the solution to

$$\frac{db}{dt} = fkD(1 - b) - glb. \tag{1}$$

Under conditions of a constant gate conformation, the time course of incorporating drug into channels is described by

$$b(t) = b(\infty) + [b(o) - b(\infty)]e^{-t/\tau}, \tag{2}$$

where

$$b(\infty) = \left(1 + \frac{gl}{fkD}\right)^{-1} \tag{3}$$

and

$$\tau = (fkD + gl)^{-1}. \tag{4}$$

When an excitable membrane is subjected to pulse train stimulation, the channel gates cycle between open and closed conformations. Let t_d be the depolarizing interval that is equivalent to the mean receptor access time and let t_r be the repolarizing interval. Under certain conditions (see Appendix), blockade associated with the nth pulse, a_n, can be described recursively in terms of blockade acquired during the previous pulse by

$$a_{n+1} = a_n e^{-\lambda} + b_d(\infty)(1 - e^{-t_d/\tau_d}) + b_r(\infty)e^{-t_d/\tau_d}(1 - e^{-t_r/\tau_r}), \tag{5}$$

where

$$\lambda = t_d/\tau_d + t_r/\tau_r \tag{6}$$

$$b_d(\infty) = \left[1 + \frac{g_d l(V_d)}{f_d kD}\right]^{-1} \tag{7}$$

$$\tau_d = [f_d kD + g_d l(V_d)]^{-1} \tag{8}$$

$$b_r(\infty) = \left[1 + \frac{g_r l(V_r)}{f_r kD}\right]^{-1} \tag{9}$$

$$\tau_r(\infty) = [f_r kD + g_r l(V_r)]^{-1} \tag{10}$$

and

$$l(V) = le^{-z\delta VF/RT}, \tag{11}$$

with δ as the fractional electrical displacement of the receptor in the membrane field.

With pulse train stimulation, Eq. 5 describes the stimulus-to-stimulus blockade and can be solved to yield a form equivalent to Eq. 2. For the nth stimulus,

$$a_n = a_{ss} + (a_o - a_{ss})e^{-\lambda n}, \tag{12}$$

where the steady state blockade, a_{ss}, is defined as

$$a_{ss} = \frac{b_d(\infty)(1 - e^{-t_d/\tau_d}) + b_r(\infty)e^{-t_d/\tau_d}(1 - e^{-t_r/\tau_r})}{1 - e^{-\lambda}}. \tag{13}$$

These theoretical results lead to three important relationships between uptake rate (Eq. 6), steady state block (Eq. 13), and stimulus interval, $I = t_d + t_r$: (*a*) use-dependent blockade follows an exponential course with uptake rate, λ; (*b*) uptake rate is a linear function of the "state"-dependent rates (τ_d^{-1} and τ_r^{-1}), which in turn are functions of the drug concentration and rate coefficients; (*c*) steady state block is a linear function of the "state"-dependent equilibria [$b_d(\infty)$ and $b_r(\infty)$]. These three results provide a test of the underlying blockade model and provide the basis of a parameter estimation procedure.

Data Analysis

Starting with use-dependent records of peak I_{Na} at several stimulus rates, we first fit each uptake curve to

$$I_{Na}(n) = I_{ss} + (I_o - I_{ss})e^{-\lambda n} \quad n = 0, 1 \ldots \tag{14}$$

where values of I_o, I_{ss}, and λ are estimated by a nonlinear least-squares procedure (Marquardt, 1963). Values of the stimulus interval, *isi*, and the associated values of λ and a_{ss} as estimated from $(I_o - I_{ss})/I_o$ are tabulated in Table I.

For a two-state model, the uptake rate is defined as

$$\lambda = (k_d D + l_d)t_d + (k_r D + l_r)t_r \tag{15}$$

$$= \lambda_d t_d + \lambda_r t_r, \tag{16}$$

where k_d, l_d, k_r, and l_r are the depolarizing and recovery state-dependent rate constants. The steady state fraction of block before depolarization is

TABLE I
ESTIMATED UPTAKE RATES AND STEADY STATE BLOCK

Stimulus interval	Pulse rate constant (λ)	a_{ss}
ms		
100	0.694	0.697
200	0.713	0.678
250	0.732	0.674
400	0.747	0.658
500	0.773	0.653
1,000	0.824	0.617
2,000	0.932	0.574
3,000	1.059	0.542
4,000	1.154	0.516
5,000	1.238	0.495
10,000	1.704	0.434

defined as

$$b_{ss} = \frac{a_\infty(1 - e^{-\lambda_d t_d})e^{-\lambda_r t_r} + b_\infty(1 - e^{-\lambda_r t_r})}{1 - e^{-\lambda}}, \quad (17)$$

while steady state block immediately after depolarization is

$$a_{ss} = \frac{b_\infty(1 - e^{-\lambda_r t_r})e^{-\lambda_d t_d} + a_\infty(1 - e^{-\lambda_d t_d})}{1 - e^{-\lambda}}, \quad (18)$$

where a_∞ and b_∞ are the depolarization and recovery state equilibria, defined as

$$a_\infty = \frac{k_d D}{k_d D + l_d}; \quad (19)$$

$$b_\infty = \frac{k_r D}{k_r D + l_r}. \quad (20)$$

From a regression of λ on t_r, values of λ_d and λ_r can be estimated by assuming a value of t_d, the mean receptor access time. Similarly, a regression based on Eq. 17 or 18 yields estimates of a_∞ and b_∞. The values of the state-dependent rates are estimated from

$$k_d = \frac{\lambda_d a_\infty}{D}; \qquad l_d = \lambda_d(1 - a_\infty); \quad (21)$$

$$k_r = \frac{\lambda_r b_\infty}{D}; \qquad l_r = \lambda_r(1 - b_\infty). \quad (22)$$

Next, we assume guard and trap functions so that the gating effects can be factored from the state-dependent rates. Assuming that block occurs in conducting channels, we let $f = m^3h$ and $g = m^3h$ and assume $m^3h = 1$ for the uptake interval. Also, we can factor the potential effect from the reverse rate coefficient by recognizing that

$$l_d = le^{-z\delta V_d F/RT} \quad (23)$$

and

$$l_r = le^{-z\delta V_r F/RT}. \quad (24)$$

The case of no m gate trapping at a resting membrane potential can be investigated by setting $f = m^3h$ and $g = h$.

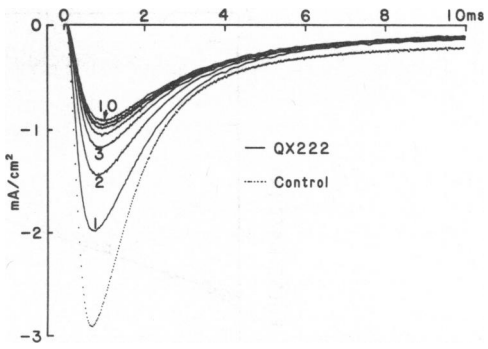

FIGURE 1 Time course of Na currents from depolarization-induced use-dependent block in the presence of 2 mM QX222. The inward currents are associated with a 0-mV test pulse. Current traces from 10 Hz stimulation are superimposed and show blockade accumulated from pulse to pulse as assessed by the reduction in I_{Na}.

RESULTS

In the presence of 2 mM QX222, peak Na current is reduced in a use-dependent manner with repetitive pulsing to 0 mV, as shown in Fig. 1. The relation between peak Na current and pulse number for three stimulus rates is plotted in Fig. 2. The relation could be fit by an exponential relationship predicted by Eq. 12, yielding the uptake rates and values of steady state blockade (see Table I). The relation between the rate constant and stimulus interval is linear (Fig. 3 *A*), as predicted from Eq. 6. From this relation, a slope and intercept are obtained that are used for calculation of state-dependent uptake rates.

The degree of use-dependent block is also frequency dependent, being enhanced with increasing frequency of stimulation, as illustrated in Fig. 2. The relationship is clearly depicted in Fig. 3 *B*, in which the equilibrium blockade is plotted as a function of $1/(1 - e^{-\lambda})$. A linear relation exists, as predicted from Eq. 13, and assuming negligible resting block ($b_r[\infty] = 0$).

From these data (Table I), we obtained least-squares

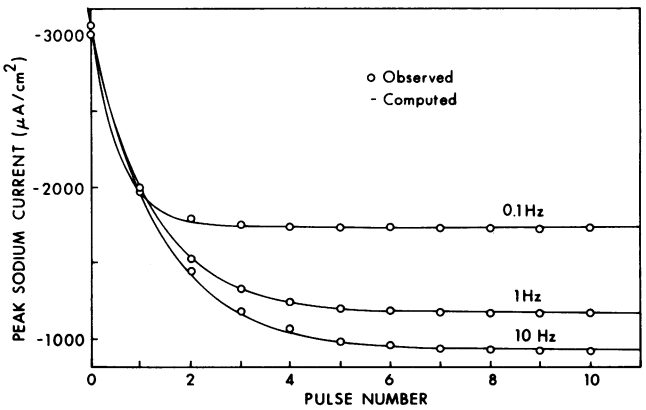

FIGURE 2 Observed (O) and computed (—) values of peak Na current at stimulus rates of 0.1, 1, and 10 Hz. The least-squares estimates of uptake rate, initial I_{Na}, and steady state I_{Na} were used to compute the predicted curve. λ = 1.704 (0.1 Hz), 0.824 (1 Hz), and 0.694 (10 Hz).

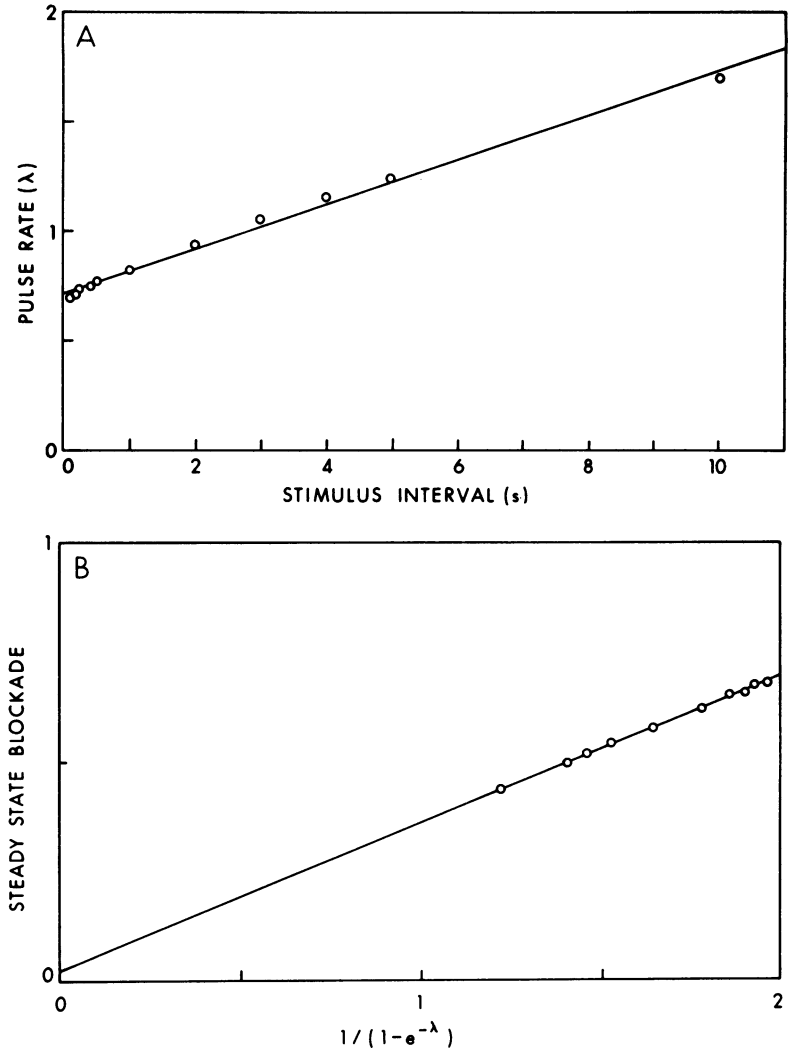

FIGURE 3 (*A*) Relationship between uptake constant, λ, and stimulus interval. With a two-voltage stimulus protocol, the time course of peak I_{Na} in the presence of a blocking agent is described by a single rate constant, λ, composed of a weighted sum of the blockade rate associated with each potential. (*B*) Relationship between steady state blockade and the pulse rate constant. Steady state peak Na current, achieved after many pulses, is related to the true equilibrium value and the stimulus interval according to

$$\text{block}_{ss} = \text{block}_{\text{equilibrium}}\, A/(1 - e^{-\lambda}).$$

estimates of $\lambda_r = 0.102$ and $\lambda_d = 715$ using Eq. 16, and $b_\infty = 0.347$ and $a_\infty = 0.687$ using Eq. 17. Assuming all binding sites would be accessible at the depolarizing potential of 0 mV ($f_d = g_d = 1$), the rate constants were $k = 2.46 \times 10^5$ $M^{-1}\,s^{-1}$, $l = 0.224 \times 10^3\,s^{-1}$. In addition, we estimated the fraction of conducting channels at −80 mV as $f_r = g_r = 7.2 \times 10^{-5}$ and the electrical location of the binding site as $\delta = 0.443$. With these parameters, Eqs. 6–11 and 17 were evaluated and Eq. 12 was used to compute predicted levels of channel blockade. For stimulus rates of 0.1, 1, and 10 Hz, the predicted and observed values of peak I_{Na} are plotted as shown in Fig. 4.

Yeh and Tanguy (1985) have demonstrated the gate-trapping effect experimentally in drug-complexed channels. This effect modifies the unblocking rate coefficient by allowing unblocking to occur only in open channels, with an apparent rate coefficient of m_r^3hl. If one assumes m gate-trapping does not occur during the recovery interval, the unblocking coefficient is hl. To illustrate the use of the steady state data as a test for trapping, we estimated rate constants assuming no trapping. From the reanalysis, we estimated $k = 3.58 \times 10^5\,M^{-1}\,s^{-1}$, and $l = 4.15 \times 10^{-3}\,s^{-1}$. Predicted peak currents (——) for three stimulus rates were computed using these values and are shown along with the observed peak currents in Fig. 5. It is readily apparent that the computed steady state values are incorrect when no trapping is assumed during the recovery interval.

Finally, we computed the recovery time constant for both trapped and untrapped models using Eq. 10. For illustrative purposes, we utilized guard and trap functions,

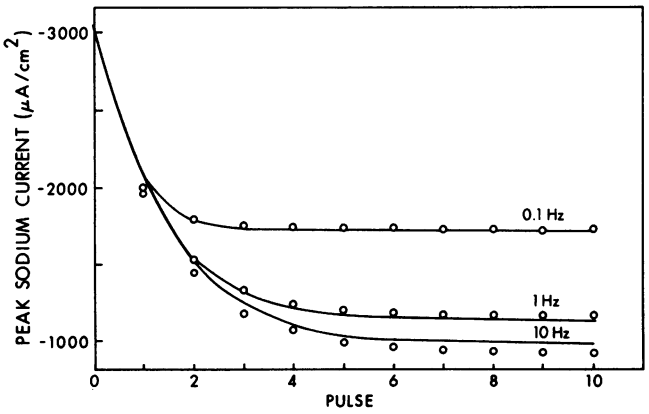

FIGURE 4 Observed (O) and predicted (—) values of peak sodium current at stimulus rates of 0.1 (top curve), 1 (middle curve), and 10 (bottom curve) Hz. For the predicted values, a single set of rate constants (k, ℓ) were utilized while the stimulus interval was varied.

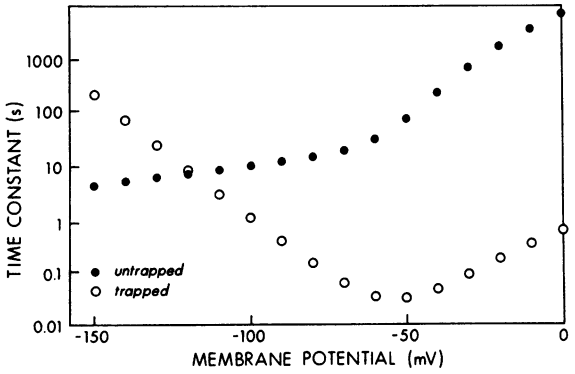

FIGURE 6 Recovery time constants as a function of membrane potential. The trapped model (O) predicts an increase in time constant with hyperpolarization, while the untrapped model (●) predicts a reduction in time constant with hyperpolarization.

f and g, defined in terms of the voltage-sensitive Hodgkin-Huxley (1952) equilibrium gating variables m_∞ and h_∞, although alternative schemes could be used. The resulting voltage-sensitive time constants are illustrated in Fig. 6. With increasing hyperpolarization, the untrapped recovery time constant continues to decrease in response to the interaction between membrane charge and the drug charge. For the trapped scheme, however, the time constant increases with increasing membrane hyperpolarization, as observed by Yeh and Tanguy (1985).

DISCUSSION

The present study demonstrates that the onset of use-dependent block follows an exponential time course in the presence of a blocking agent that specifically blocks conducting Na channels. By considering pulse train stimulation as switching the binding site between an accessible and inaccessible conformation, we have developed an analytical model that predicts that use-dependent blockade should follow an exponential time course, that the rate of the time course is a linear function of the state-dependent rates, and that the steady state block reached after many pulses is a linear function of the state-dependent blockade equilibria. Thus, we have established a theoretical tie between the theories of continuously accessible receptors and periodically accessible receptors.

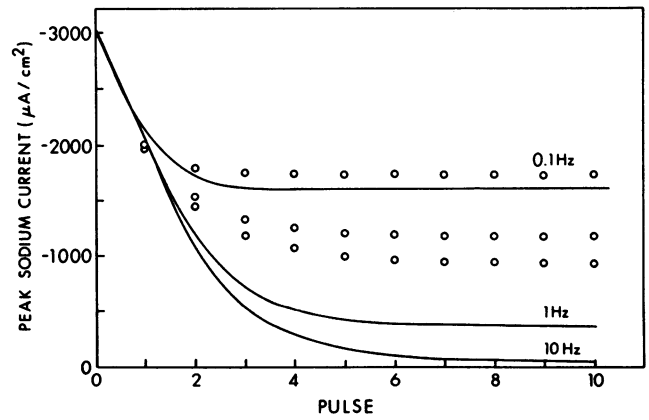

FIGURE 5 Computed and observed peak I_{Na} values for 0.1, 1, and 10 Hz stimulation with 2 mM QX222. The rate constants were estimated assuming no gate trapping of drug within the channel. This model gives a poor fit as shown by overestimation of steady state blockade.

Ligand-receptor interactions in which ligands have continuous access to the receptor binding site have been characterized by a bimolecular binding process. By observing the process under a fixed condition or "state," one can estimate forward and reverse rate constants from data describing the observed time course of binding (time constant) and the observed equilibrium fractions of bound receptors (equilibrium block).

This approach has been successfully applied to analyzing the blocking action of tetraethylammonium derivatives on the K channel, as was pioneered by Armstrong (1969, 1971), and elaborated by French and Shoukimas (1981) and Swenson (1981). The continuous access of the blocking agent to the receptor binding site could be approximated in the case of K channels, because the channel does not undergo inactivation during a maintained depolarizing pulse. Thus, in the absence of a blocking agent, the K current is turned on in response to membrane depolarization and maintained during the whole duration of depolarization pulse. In the presence of some blocking agents, the K current is still turned on normally, reaches a peak, and then starts to decay exponentially to a steady state value. From the time constant, estimated from the decaying phase, and the equilibrium block, calculated from the ratio of steady state values in the absence and in the presence of the blocking agent, one can estimate forward and reverse rate constants governing the interaction of the blocking agent with open K channels.

Such an analysis is not entirely appropriate for characterizing Na channel blockade, because the channel inacti-

vates over the time course of the depolarizing potential, thereby limiting the time available to reach blockade equilibrium. As a result, the time course of the Na current decay owing to the channel inactivation cannot be differentiated from the time course of the decay owing to the drug's blocking action. One way to circumvent this complication is to remove the Na inactivation, making the Na channel behave as the K channel. Using this approach, the rate constants governing the drug-Na channel interaction have been estimated for pancuronium (Yeh and Narahashi, 1977), 9-aminoacridine (Cahalan, 1978; Yeh, 1982; Yeh and Oxford, 1985), and methylene blue (Starkus et al., 1984). Using the rate constants extracted from the 9-aminoacridine block of the Na channel in the pronase-treated axon, Yeh and Oxford (1985) have been able to simulate the use-dependent block of the Na current observed in the inactivation intact axon. However, this approach is of limited utility for most local anesthetics (including lidocaine, QX222, and QX314), because these agents probably modify the blocking process (Yeh, 1978; Cahalan, 1978).

So far, two methods have been used to characterize the rate constants governing the drug blocking action on Na channels. Using a simplified three-state kinetic model, Schwarz et al. (1977) estimated three sets of rate constants by trial and error to imitate use-dependent block of peak Na current in the presence of lidocaine. An alternative method is to incorporate a gating model for the Na channel activation and inactivation processes into the rate constants. Using these composite rate constants, Courtney and his associates (Courtney et al., 1978; Courtney, 1980) developed a difference-differential equation to approximate use-dependent block. Both forward and reverse rate constants governing the open channel block were found to be several 100–1,000-fold as large as those governing the resting block. Starmer et al. (1984) developed a simpler differential equation that was based on the guarded-receptor model, a special case of the modulated-receptor model. Only one set of rate constants was estimated and sufficed to simulate use-dependent block. The apparent profound difference in the rate of drug binding to open channels and to resting channels, in their view, is attributed to the accessibility of the receptor, which is controlled by the Na channel gates. In this paper, this gate-trapping mechanism has been incorporated into the present analysis. With this provision, the unblocking rate constant at rest (-80 mV) is estimated to be on the order of 1 ms^{-1}. This new value is several 1,000-fold larger than the value previously estimated (Courtney, 1978, 1980; Starmer et al., 1984), but is within ranges that have been estimated using the continuous model for the agents that are capable of blocking open channels in the pronase-treated axon (Yeh and Narahashi, 1977; Cahalan and Almers, 1979; Yeh and Oxford, 1985).

Characterization of channel blocking agents, particularly for channels that inactivate, would be considerably enhanced if a simple procedure for estimating binding and unbinding rates could be developed. With the H-H gating model, the models of Strichartz (1973), Courtney (1975), Hondeghem and Katzung (1977), Yeh (1982), and Starmer et al. (1984) did not readily admit to simplification. However, a hint of a strategy for simplifying the gating model is provided by single channel observations.

Suppose we assume an ensemble of channels where all the channels open immediately upon depolarization and remain open for an interval equal to the mean channel open time. (We also ignore the interval between the end of the channel open interval and the end of the stimulating pulse interval.) The trap and guard functions then become constant during the channel open time and the recovery time. The errors encountered by this simplification ought to be small. For many stimulus protocols, the channel open time is small in comparison with the stimulus interval (1:100 at 10 Hz). The time to first opening is similarly small in contrast to the stimulus interval, as is the time between channel closure and the end of the depolarization interval. Ignoring these stochastic variations thus seems reasonable. The resultant model based on synchronized gating is functionally equivalent to that describing continuous ligand-receptor interactions for two conditions, uptake and recovery. This similarity provides a means for comparing equilibrium ligand-binding experiments with pulse-train–promoted ligand-binding experiments, for as the uptake time (channel open time) increases, a_{ss} becomes equivalent to the equilibrium fraction of blocked channels, $b(\infty)$.

A sensitive test for discriminating among several blockade models can be based on the time course of blockade recovery as a function of membrane holding potential. There are three primary classes of models: *m* gate-trapped agents, *m* gate-untrapped agents, and agent-induced modification in inactivation kinetics. For these three models, one would expect the recovery time constants to increase with hyperpolarizing potentials for *m* gate-trapped agents, to decrease with *m* gate-untrapped agents, and to show no voltage sensitivity for potentials where h^* (modified inactivation gates) = 1. Yeh and Tanguy (1985) recently showed an *e*-fold increase in recovery time constant for each 14-mV reduction in holding potential, which provides additional support for the *m* gate-trapping hypothesis. Accordingly, we simulated the time constant of recovery as a function of holding potential for both the trapped and untrapped hypothesis. We used Hodgkin-Huxley gating kinetics for the computation. As shown in Fig. 6, the recovery time constant from trapped drug increases for both hyperpolarizing and depolarizing potentials, with a minimum in the region of -50 mV. For untrapped drug, however, the recovery time constant varies monotonically with membrane potential, illustrating both potential effects for $V_{membrane} < -60$ mV and combined potential and gating effects for $V \geq -60$ mV.

With the quaternary lidocaine derivative QX222, we

have shown that a bimolecular model of a transiently accessible binding site is adequate to account for the use- and frequency-dependent patterns of peak Na current. Furthermore, we have shown the equivalence between rate constants characterizing transiently accessible binding sites and rate constants characterizing continuously accessible binding sites. This provides a means for comparing the results of labeled ligand binding studies with the results of blockade assessed electrophysiologically. Equally important, this model demonstrates the coupling between unobserved state-specific binding parameters and the observed uptake rate and steady state block.

APPENDIX

Derivation of Blockade with Repetitive Stimulation

The underlying model of channel blockade is considered a bimolecular process relating unblocked channels, U, drug, D, and blocked channels, B. We postulate that the channel gates control migration of drug between the channel binding site and drug pools. In particular, we define a fraction, f, of the unblocked channels where drug can readily diffuse from a pool to the binding site (unguarded sites) and a fraction of blocked channels, g, where drug can unbind and readily diffuse away from the binding site (untrapped drug). Schematically,

$$\mathrm{U} + \mathrm{D} \underset{gl}{\overset{fk}{\rightleftharpoons}} \mathrm{B}.$$

With pulse train stimulation, we assume that shifts in stimulus potential induce shifts in unblocked channel binding sites between guarded and unguarded status. Similarly, in drug-complexed channels, the bound receptors shift between trapped and untrapped status. We assume the transition between states is fast, so the blockade process at a particular stimulus potential can be described by

$$b(t) = b_\infty + (b(o) - b_\infty)\mathrm{e}^{-t/\tau}, \tag{A1}$$

where

$$b_\infty = \left(1 + \frac{gl}{fkD}\right)^{-1}, \quad \tau = (fkD + gl)^{-1}, \tag{A2}$$

and the guard and trap functions, f and g, are assumed to be voltage sensitive.

We note that when pulse-train stimulation is used to induce blockade, the blockade at the beginning of a potential is equal to the blockade at the end of the previous potential. In other words, blockade can be described recursively in terms of blockade acquired during the prior pulse. To illustrate, we divide each stimulus into intervals of constant potential. For many protocols, this amounts to switching between depolarizing and recovery potentials, V_d and V_r, with durations t_d and t_r. For the uptake interval, we use the mean channel open time, t_o, instead of the actual depolarization interval. We also ignore the interval between channel closure and the end of depolarization. For exponentially distributed open times, this results in a first-order approximation of the true expected value of blockade (Starmer and Grant, 1985).

Let b_0 represent the initial fraction of blocked channels, b_n represent the block before the nth stimulus, and a_n represent the block after the nth stimulus. Blockade associated with each pulse of the train is thus described by

$$b_0 \text{ (initial condition)} \tag{A3}$$

$$a_0 = a_\infty + (b_0 - a_\infty)\mathrm{e}^{-t_d/\tau_d} \tag{A4}$$

$$b_1 = b_\infty + (a_0 - b_\infty)\mathrm{e}^{-t_r/\tau_r} \tag{A5}$$

$$a_1 = a_\infty + (b_1 - a_\infty)\mathrm{e}^{-t_d/\tau_d} \tag{A6}$$

$$\vdots$$

$$a_n = a_\infty + (b_n - a_\infty)\mathrm{e}^{-t_d/\tau_d} \tag{A7}$$

$$b_{n+1} = b_\infty + (a_n - b_\infty)\mathrm{e}^{-t_r/\tau_r}. \tag{A8}$$

Substituting

$$a_n = a_{n-1}\mathrm{e}^{-(t_d/\tau_d + t_r/\tau_r)} + b_\infty(1 - \mathrm{e}^{-t_r/\tau_r})\mathrm{e}^{-t_d/\tau_d} + a_\infty(1 - \mathrm{e}^{-t_d/\tau_d}); \tag{A9}$$

$$b_{n+1} = b_n\mathrm{e}^{-(t_d/\tau_d + t_r/\tau_r)} + a_\infty(1 - \mathrm{e}^{-t_d/\tau_d})\mathrm{e}^{-t_r/\tau_r} + b_\infty(1 - \mathrm{e}^{-t_r/\tau_r}). \tag{A10}$$

Define the uptake rate, λ, as

$$\lambda = t_d/\tau_d + t_r/\tau_r \tag{A11}$$

and constants A and B as

$$A = b_\infty(1 - \mathrm{e}^{-t_r/\tau_r})\mathrm{e}^{-t_d/\tau_d} + a_\infty(1 - \mathrm{e}^{-t_d/\tau_d}); \tag{A12}$$

$$B = a_\infty(1 - \mathrm{e}^{-t_d/\tau_d})\mathrm{e}^{-t_r/\tau_r} + b_\infty(1 - \mathrm{e}^{-t_r/\tau_r}). \tag{A13}$$

The blockade for the nth pulse then becomes

$$a_n = a_{n-1}\mathrm{e}^{-\lambda} + A; \tag{A14}$$

$$b_n = b_{n-1}\mathrm{e}^{-\lambda} + B. \tag{A15}$$

After many pulses, a steady state is reached where $a_n = a_{n-1}$ and $b_n = b_{n-1}$, so the steady state blockade, a_{ss} and b_{ss}, become

$$a_{ss} = \frac{A}{1 - \mathrm{e}^{-\lambda}}; \tag{A16}$$

$$b_{ss} = \frac{B}{1 - \mathrm{e}^{-\lambda}}. \tag{A17}$$

The solutions of Eqs. A14 and A15 are

$$a_n = a_{ss} + (a_0 - a_{ss})\mathrm{e}^{-n\lambda}; \tag{A18}$$

$$b_n = b_{ss} + (b_0 - b_{ss})\mathrm{e}^{-n\lambda}. \tag{A19}$$

This work was supported by grants HL32994, RR01693, and GM24866 from the National Institutes of Health.

Received for publication 29 May 1985 and in final form 25 October 1985.

REFERENCES

Armstrong, C. M. 1969. Inactivation of the potassium conductance and related phenomena caused by quaternary ammonium ion injection in squid axons. *J. Gen. Physiol.* 54:553–575.

Armstrong, C. M. 1971. Interaction of tetraethylammonium ion deriva-

tives with the potassium channels of giant axons. *J. Gen. Physiol.* 58:413–437.

Baker, P. F., A. L. Hodgkin, and T. I. Shaw. 1961. Replacement of the protoplasm of a giant nerve fiber with artificial solutions. *Nature (Lond.).* 190:885–887.

Cahalan, M. D. 1978. Local anesthetic block of sodium channels in normal and pronase-treated squid giant axons. *Biophys. J.* 23:285–311.

Cahalan, M. D., and W. Almers. 1979. Block of sodium conductance and gating current in squid giant axons poisoned with quaternary strychnine. *Biophys. J.* 27:57–73.

Courtney, K. R. 1975. Mechanism of frequency-dependent inhibition of sodium currents in frog myelinated nerve by the lidocaine derivative GEA 968. *J. Pharmacol. Exp. Ther.* 195:225–236.

Courtney, K. R. 1980. Structure-activity relations for frequency-dependent sodium channel block in nerve by local anesthetics. *J. Pharmacol. Exp. Ther.* 213:114–119.

Courtney, K. R., J. J. Kendig, and E. N. Cohen. 1978. The rates of interaction of local anesthetics with sodium channels in nerve. *J. Pharmacol. Exp. Ther.* 207:594–604.

French, R. J., and J. J. Shoukimas. 1981. Blockage of squid axon potassium conductance by internal tetra-n-alkylammonium ions of various sizes. *Biophys. J.* 34:271–291.

Hille, B. 1977. Local anesthetics: hydrophilic and hydrophobic pathways for the drug-receptor reaction. *J. Gen. Physiol.* 69:497–515.

Hodgkin, A. L., and A. F. Huxley. 1952. A quantitative description of membrane current and its application to conduction and excitation in nerve. *J. Physiol. (Lond.).* 117:500–544.

Hondeghem, L. M., and B. G. Katzung. 1977. Time- and voltage-dependent interactions of antiarrhythmic drugs with cardiac sodium channels. *Biochim. Biophys. Acta.* 472:1–26.

Marquardt, D. W. 1963. An algorithm for least-squares estimation of non-linear parameters. *J. Soc. Ind. Appl. Math.* 11:431–441.

Oxford, G. S. 1981. Some kinetic and steady-state properties of sodium channels after removal of inactivation. *J. Gen. Physiol.* 77:1–22.

Schwarz, W., P. T. Palade, and B. Hille. 1977. Effects of pH on use-dependent block of Na channels in frog muscle. *Biophys. J.* 20:343–368.

Starkus, J. G., S. T. Heggeness, and M. D. Rayner. 1984. Kinetic analysis of sodium channel block by internal methylene blue in pronased crayfish giant axons. *Biophys. J.* 46:205–218.

Starmer, C. F., and A. O. Grant. 1985. Phasic ion channel blockade—a kinetic model and estimation procedure. *Mol. Pharmacol.* 28:348–356.

Starmer, C. F., A. O. Grant, and H. C. Strauss. 1984. Mechanisms of use-dependent block of sodium channels in excitable membranes by local anesthetics. *Biophys. J.* 46:15–27.

Starmer, C. F., and M. D. Hollett. 1985. Mechanisms of apparent affinity variation of guarded receptors. *J. Theor. Biol.* 115:337–349.

Strichartz, G. R. 1973. The inhibition of sodium currents in myelinated nerve by quaternary derivatives of lidocaine. *J. Gen. Physiol.* 62:37–57.

Swenson, R. P., Jr. 1981. Inactivation of potassium currents in squid axon by a variety of quaternary ammonium ions. *J. Gen. Physiol.* 77:255–271.

Yeh, J. Z. 1978. Sodium inactivation mechanism modulates QX-314 block of sodium channels in squid axons. *Biophys. J.* 24:569–574.

Yeh, J. Z., and T. Narahashi. 1977. Kinetic analysis of pancuronium interaction with sodium channels in squid axon membrane. *J. Gen. Physiol.* 69:293–323.

Yeh, J. Z. 1979. Dynamics of 9-aminoacridine block of sodium channels in squid axons. *J. Gen. Physiol.* 73:1–21.

Yeh, J. Z. 1982. A pharmacological approach to the structure of the Na channel in squid axon. *In* Proteins in the Nervous System: Structure and Function. B. Haber, J. R. Perez-Polo, and J. D. Coulter, editors. Alan R. Liss, New York. 17–49.

Yeh, J. Z., and G. S. Oxford. 1985. Interactions of monovalent cations with sodium channels in squid axon. II. Modification of pharmacological inactivation gating. *J. Gen. Physiol.* 85:603–620.

Yeh, J. Z., and J. Tanguy. 1985. The Na channel activation gate modulates slow recovery from use-dependent block by local anesthetics in squid giant axons. *Biophys. J.* 47:685–694.